Original Article

JCBFM

Journal of Cerebral Blood Flow & Metabolism
2016, Vol. 36(8) 1424–1433
© Author(s) 2015
Reprints and permissions:
sagepub.co.uk/journalsPermissions.nav
DOI: 10.1177/0271678X15606713
jcbfm.sagepub.com

SAGE

Oxygen extraction fraction measurement using quantitative susceptibility mapping: Comparison with positron emission tomography

Kohsuke Kudo[1,2], Tian Liu[3,4], Toshiyuki Murakami[5], Jonathan Goodwin[1], Ikuko Uwano[1], Fumio Yamashita[1], Satomi Higuchi[1], Yi Wang[3], Kuniaki Ogasawara[5], Akira Ogawa[5] and Makoto Sasaki[1]

Abstract

The purposes of this study are to establish oxygen extraction fraction (OEF) measurements using quantitative susceptibility mapping (QSM) of magnetic resonance imaging (MRI), and to compare QSM–OEF data with the gold standard ^{15}O positron emission tomography (PET). Twenty-six patients with chronic unilateral internal carotid artery or middle cerebral artery stenosis or occlusion, and 15 normal subjects were included. MRI scans were conducted using a 3.0 Tesla scanner with a three-dimensional spoiled gradient recalled sequence. QSM images were created using the morphology-enabled dipole inversion method, and OEF maps were generated from QSM images using extraction of venous susceptibility induced by deoxygenated hemoglobin. Significant correlation of relative OEF ratio to contra-lateral hemisphere between QSM–OEF and PET–OEF was observed ($r = 0.62$, $p < 0.001$). The local (intra-section) correlation was also significant ($r = 0.52$, $p < 0.001$) in patients with increased PET–OEF. The sensitivity and specificity of OEF increase in QSM was 0.63 (5/8) and 0.89 (16/18), respectively, in comparison with PET. In conclusion, good correlation was achieved between QSM–OEF and PET–OEF in the identification of elevated OEF in affected hemispheres of patients with unilateral chronic steno-occlusive disease.

Keywords

Cerebral ischemia, magnetic resonance imaging, oxygen extraction fraction, positron emission tomography, quantitative susceptibility mapping

Received 27 January 2015; Revised 23 July 2015; Accepted 3 August 2015

Introduction

Oxygen extraction fraction (OEF) represents an important measurable parameter of brain metabolism,[1] which can provide information about the relative deficiencies in cerebral blood supply with the tissue's demand for oxygen, so called misery perfusion.[2] The risk of stroke recurrence increases with misery perfusion in patients with symptomatic major cerebral arterial occlusive disease.[3,4] Positron emission tomography (PET) is generally considered to be the gold standard approach for OEF measurements; however, PET has several disadvantages such as limited availability and radiation exposure.

Recent advancement in the field of magnetic resonance (MR) imaging has seen the introduction of several new approaches to OEF measurement. One of these approaches relies on the measurement of T2* or T2'

[1]Division of Ultra-High Field MRI, Iwate Medical University, Japan
[2]Department of Diagnostic and Interventional Radiology, Hokkaido University Hospital, Japan
[3]Departments of Radiology, Weill Cornell Medical College, New York, NY, USA
[4]MedImageMetric LLC, New York, NY, USA
[5]Department of Neurosurgery, Iwate Medical University, Japan

Corresponding author:
Kohsuke Kudo, Department of Diagnostic and Interventional Radiology, Hokkaido University Hospital, N14 W5 Kita-ku, Sapporo 060-8648, Japan.
Email: kkudo@huhp.hokudai.ac.jp

relaxation associated with the presence of paramagnetic deoxygenated hemoglobin (deoxy-Hb) in brain tissue (blood oxygen dependent level, BOLD) to measure tissue OEF.[5–8] An alternative method utilizing a spin tagging technique has been developed, allowing quantification of OEF based on the measurement of T2 relaxation in venous blood.[9,10] However, most applications in these techniques were only for normal subjects, and there were few patient's studies.[11] In addition, few studies reported reproducibility and dynamic changes under physiological or pharmacological challenges.[12]

A method utilizing phase differences between the venous blood and surrounding tissue to calculate venous oxygen saturation and OEF[13,14] has also shown to be a potential viable approach; however, this method enables an estimate of the relative change in OEF (ΔOEF) based on the comparison of two separate images, rather than absolute measurements in OEF. To date few of these previously developed magnetic resonance imaging (MRI)-based approaches to OEF measurement has been applied to a clinical cohort where cerebrovascular function is likely to be compromised, therefore, uncertainty remains as to the viability of these methods as a potential alternative to PET.

Quantitative susceptibility mapping (QSM) is a novel post-processing technique, which yields quantitative measurement of magnetic susceptibility from a single MRI phase image acquisition.[15] Compared to previous venous phase-based MRI techniques, which require two separate scans and only allow an estimate of relative change in OEF (ΔOEF), the QSM technique is insensitive to the geometry of veins and dipolar artifacts; both of which affect the measured distribution of measured phase values. As a result of this insensitivity, we expect that absolute quantification of OEF by measuring venous concentration of deoxy-Hb can be obtained with a single data acquisition.

The purposes of this study are (a) to establish a method for OEF calculation and map creation based on QSM technique of MRI, and (b) to compare OEF between QSM and gold standard ^{15}O-PET in patients with unilateral chronic steno-occlusive disease.

Materials and methods

Subjects

From April 2010 to September 2011, 29 patients who were admitted to our hospital for pre-operative evaluation of unilateral chronic major cerebral artery steno-occlusive disease were selected for this study. Three of these patients were excluded based on past history of subcortical hemorrhage shown on susceptibility weighted imaging (SWI), which has the potential to disrupt QSM calculation due to strong susceptibility effects associated with iron within blood breakdown products such as hemosiderin. Finally, 26 patients (seven females and 19 males) with chronic unilateral internal carotid or middle cerebral artery (ICA or MCA, respectively) stenosis or occlusion were eligible for this study. Their ages ranged from 39 to 77 (mean 63.6) years. Eleven patients had ICA occlusion and 15 patients had MCA stenosis or occlusion (eight stenosis and seven occlusion). These patients underwent both MRI and PET scans with a mean interval of 10 days. Fifteen normal subjects (two female and 13 males) were also added for the determination of normal range of QSM-OEF and the intra-subject reproducibility. Their ages ranged from 21 to 44 (mean 31.1) years. They were confirmed to have no past history of neurological diseases.

The study protocol was reviewed and approved by the Institutional Review Board at the Iwate Medical University and written informed consent was obtained from all participants prior to enrollment in the study.

MRI

MRI scans were conducted using a 3.0 Tesla scanner (Signa HDxt, GE Healthcare, Milwaukee, USA) with a quadrature head coil. A three-dimensional (3D) spoiled gradient recalled (SPGR) sequence with flow compensation was used for phase image acquisition. The scan parameters included a flip angle of 18 degree, echo time (TE) of 30 ms, repetition time (TR) of 44 ms, number of excitations of 1, field of view (FOV) of 256 mm, slice thickness of 2 mm, number of partitions of 30, acquisition matrix of 384×160, and a reconstruction matrix of 512×512. The scan time was 3 min and 3 s. The imaging slab was set from the level of the basal ganglia to the high convexity. The magnitude, real, and imaginary images were reconstructed.

QSM images were created using the morphology-enabled dipole inversion (MEDI) method.[15,16] This method uses phase derived from real and imaginary images to measure the magnetic field inhomogeneity, which can then be inverted to obtain an estimate of the underlying susceptibility distribution. Despite there being more than one possible mathematical solution for the calculated susceptibility distribution, a susceptibility map can be uniquely determined by taking advantage of the morphological prior information of the brain obtained from the same data acquisition. In this work, this MEDI approach was used to generate

the middle twenty-five QSM images from thirty slices of source data.

OEF maps were generated from QSM images by using a similar method in the previous article (Figure 1).[14] Firstly, a venous mask was created using a local threshold method with a volume-of-interest (VOI) of $50 \times 50 \times 50$ mm ($100 \times 100 \times 25$ voxels). A local threshold value of mean +2 standard deviations (SD) was used for the segmentation of venous voxels in the VOI, based on the idea that the susceptibility of vein becomes higher than brain parenchyma due to the elevated level of deoxy-Hb. After segmentation of venous pixels (Figure 1b), the susceptibility difference ($\Delta\chi$) between the average susceptibility of veins and surrounding tissue was calculated in each VOI. An estimate of oxygen saturation (Y) can be obtained using following equation

$$\Delta\chi = \Delta\chi_{do} \times \mathrm{Hct} \times (1 - Y) \quad (1)$$

where $\Delta\chi_{do}$ (1.8×10^{-7} in CGS units) is the susceptibility difference per unit hematocrit (Hct) between fully deoxygenated blood and fully oxygenated blood.[17] We assumed an Hct value of 0.45. For the correction of partial volume effects, we assumed an average diameter for cortical veins of 1 mm.[18] And in accordance with a previous study,[19] we applied a correction factor for partial volume effects (Pv), which was measured as approximately 7.0 when a voxel ratio of 1:4

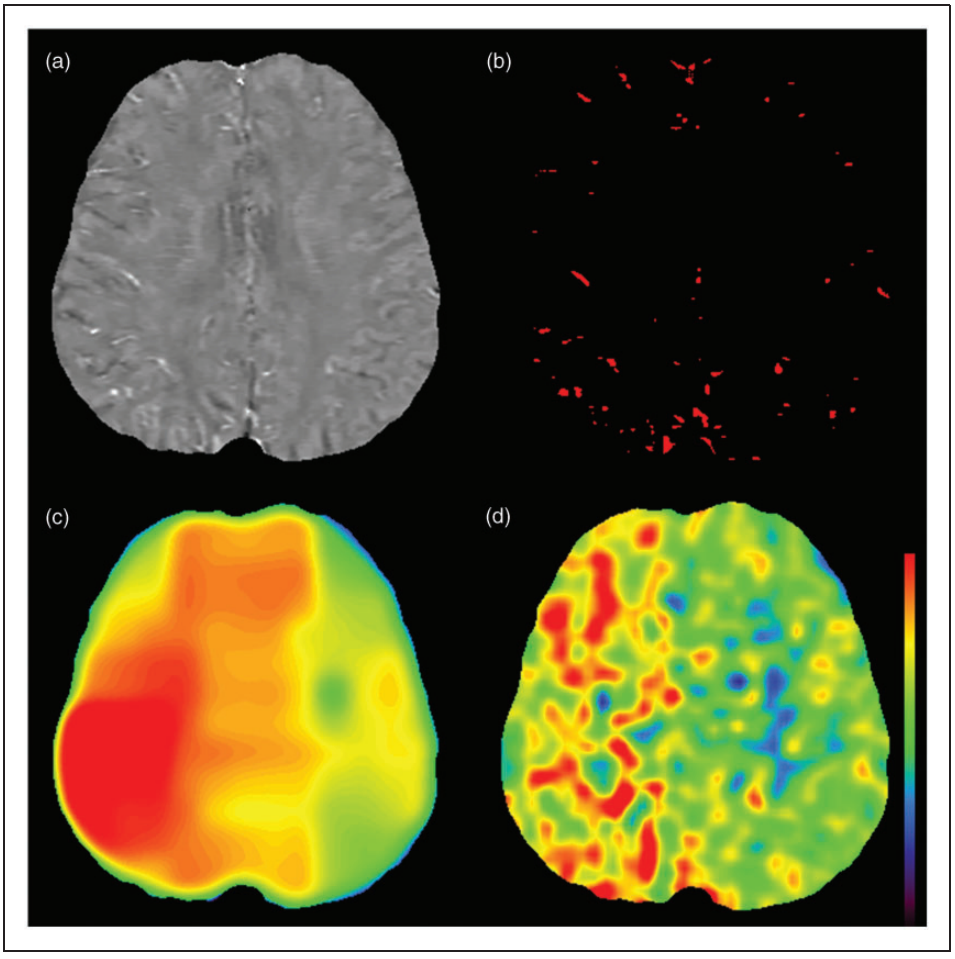

Figure 1. Creation of oxygen extraction fraction (OEF) map. Quantitative susceptibility map (QSM) in patient of right internal carotid artery occlusion (73-year-old male) is shown (a). Bright veins in the right hemisphere are noted, which indicates increased amount of deoxygenated hemoglobin. Venous mask image (b) is obtained by using local threshold method. Oxygen extraction fraction (OEF) map (c) is created from susceptibility value of these veins. Increased OEF is observed in the right hemisphere, which corresponds well to OEF map of PET (d). The same color scale is used both for QSM-OEF and PET-OEF.

was applied, with a vessel diameter equivalent to 2 pixels.

$$\Delta\chi = \Delta\chi_{do} \times \mathrm{Hct} \times (1 - Y) \times \frac{1}{pv} \quad (2)$$

Under normal respiratory conditions, arterial oxygen saturation is stable and assumed to be nearly 100%. Consequently, OEF can be approximately related to venous oxygen saturation only,[20] using the following relationship

$$\mathrm{OEF} = 1 - \mathrm{Y} \quad (3)$$

In each above-mentioned VOI, OEF value from vessels was calculated, which represented the mean OEF value of the VOI. Then, the above-mentioned VOI was applied to whole images by sliding the VOI with increments of 12.5 mm (sliding window method) in X and Y directions, allowing OEF maps to be generated on a slice-by-slice basis.

Positron emission tomography

PET scans were performed using a SET-3000GCT/M scanner (PET/CT; Shimadzu Corp, Kyoto, Japan) with gadolinium silica oxide detectors. The axial field of view was 256 mm and in-plane spatial resolution was 3.5-mm full width at half maximum. Fifty-nine slices with 2.6-mm slice thickness were scanned and axial spatial resolution was 4.2-mm full width at half maximum. The scanner was operated in a static scan mode with dual energy window acquisition for scatter correction. The coincidence time window was set to 10 ns. Before emission scans, a transmission scan (3 min) with a ^{137}Cs point source was performed using a bismuth germinate transmission detector ring coaxially attached to the gadolinium silica oxide emission detector ring. OEF measurement was performed for 5 min during continuous inhalation of $^{15}O_2$ (1480 MBq), while a single breath of C^{15}O (444 MBq) was used to measure CBV. Ordered subset expectation maximization (OSEM) algorithm was used for image reconstruction. OEF was calculated using the steady-state method with correction by CBV.[21]

Data processing of OEF

Co-registration of PET-OEF and QSM-OEF images was performed using MRI magnitude images and SPM8 software (http://www.fil.ion.ucl.ac.uk/spm/). The registered QSM-OEF and PET-OEF images were then imported into a freely available software (Perfusion Mismatch Analyzer, PMA, version 4.0.4),[22] where automated measurement of regions-of-interest (ROIs) was performed using a previously described method.[22,23] On a slice at the level of central semiovale, 18 spherical ROIs with a diameter of 10 mm (20 pixels) were automatically placed along the entire parenchymal surface of the brain, without overlapping each other (Figure 2). As we performed registration between QSM and PET before ROI measurement, the same locations were measured between QSM and PET.

Statistical analysis

The mean OEF value of each hemisphere (average of 9 ROIs for each hemisphere) for all patients was calculated for QSM-OEF and PET-OEF images. The mean OEF of each hemisphere in normal subjects was also calculated for QSM-OEF. Differences in mean OEF of patients between affected and contralateral sides and between QSM-OEF and PET-OEF were compared with a paired t-test, respectively.

Then, OEF ratio in patients was calculated for each of QSM-OEF and PET-OEF

$$\mathrm{OEF\_Ratio} = \frac{OEF_{affected}}{OEF_{contraiteral}} \quad (4)$$

In order to define normal range of QSM-OEF ratio, mean and SD of 15 normal subjects were calculated. Then, increased QSM-OEF was defined as OEF ratio

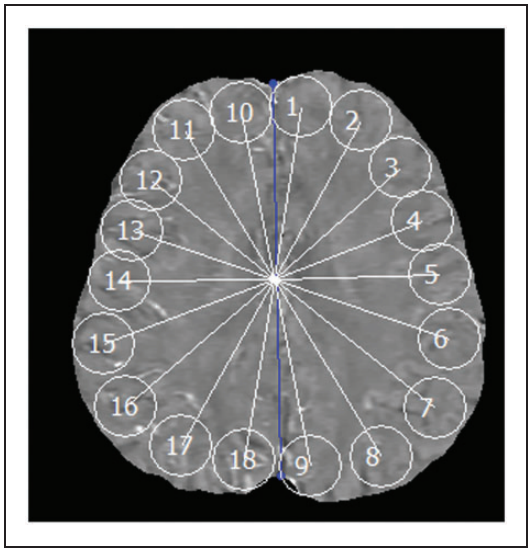

Figure 2. Region-of-interest (ROI) measurements.example of automated measurement of region-of-interest (ROI) is shown. Eighteen spherical ROIs are automatically placed along the entire parenchymal surface of the brain. Blue line indicates midline of the brain.

Table 1. Absolute OEF values.

		PET-OEF			QSM-OEF		
		mean	±	SD	mean	±	SD
Patients	Affected side	47.9	±	8.4	55.5	±	7.8
	Contralateral side	45.2	±	7.2	53.2	±	9.0
Normal Subjects		N.A.			49.8	±	4.8

PET: positron emission tomography; OEF: oxygen extraction fraction; QSM: quantitative susceptibility mapping; SD: standard deviation; N.A.: not applicable.

Table 2. Number of patients who had increased/preserved OEF.

		QSM-OEF		
		Increased	Preserved	Total
PET-OEF	Increased	5	3	8
	Preserved	2	16	18
	Total	7	19	26

PET: positron emission tomography; OEF: oxygen extraction fraction; QSM: quantitative susceptibility mapping.

above mean + 2SD. Increased PET-OEF was also defined by mean + 2SD (1.09) from previous reports.[24] The numbers of increased or preserved OEF were counted for QSM and PET, and Fisher exact test was used for the statistical test. The sensitivity and specificity of QSM-OEF to predict increased OEF were also calculated (based on PET-OEF).

Correlation of OEF ratio between QSM-OEF and PET-OEF for all patients was assessed by linear regression analysis and Pearson's correlation coefficient. Bland-Altman graph was also used for the evaluation of systemic biases.

Local (intra-section) correlation between QSM-OEF and PET-OEF was also analyzed with Pearson's correlation coefficient using all 18 ROIs for each patient. The mean correlation coefficient was then calculated for all patients, as well as for the increased PET-OEF group and preserved PET-OEF group. The correlation coefficients of these two groups were compared with Mann-Whitney U-test. The linear regression analysis was also performed using all ROI data (18 ROIs for each patient), for increased PET-OEF group and preserved PET-OEF group, respectively.

For the assessment of intra-subject reproducibility, two normal subjects (28-year-old male and 44-year old male) were scanned twice with the interval of one week. Intra-class correlation (ICC) was calculated using 18 ROIs for each subjects.

Data are shown as mean ± SD when applicable. A p value less than 0.05 was considered significant in all statistical tests.

Results

The OEF values are summarized in Table 1. PET-OEF in the affected hemisphere (47.9 ± 8.4) was significantly higher than that in the contralateral hemisphere (45.2 ± 7.2) ($p = 0.006$). In QSM, OEF value in the affected hemisphere (55.5 ± 7.8) was also higher than that in the contralateral hemisphere (53.2 ± 9.0); however, the difference was not significant ($p = 0.07$). In the comparison between PET-OEF and QSM-OEF, the differences were statistically significant both for affected ($p < 0.001$) and contralateral sides ($p < 0.001$).

The mean and SD of QSM-OEF ratio in normal subjects were 1.00 and 0.06, respectively. Then, the upper limit of normal range (mean + 2SD) in QSM-OEF was defined as 1.12. The upper limit of normal range (mean + 2SD, 1.09) in PET-OEF was taken from the previous report.[24] According to these data, eight patients had increased PET-OEF, in which five had increased QSM-OEF and three had preserved QSM-OEF (Table 2). Eighteen patients had preserved PET-OEF, and among them, two had increased QSM-OEF and 16 had preserved QSM-OEF. Fisher exact test revealed that the relationship was statistically significant ($p = 0.014$). The sensitivity of QSM-OEF was 0.63 (5/8) and the specificity was 0.89 (16/18).

The scatter plot of OEF ratio between QSM and PET is shown in Figure 3. The correlation was statistically significant ($p < 0.001$) and Pearson's correlation coefficient (r) was 0.62, indicating good correlation. The slope and intercept for linear regression analysis were 0.65 and 0.37, respectively. The Bland-Altman graph shows most of the data were within mean ± 2SD, and there was no systemic bias (Figure 4).

The average local (intra-section) correlation coefficients for all patients was 0.13 ± 0.29 (Table 3). The correlation coefficients of the increased PET-OEF group (r = 0.31 ± 0.28) was significantly higher than that of the preserved OEF group (r = 0.05 ± 0.26) ($p = 0.030$). In the scatter plot of local correlation with all the ROI data (18 ROIs per patient, Figure 5), significant and moderate correlation is observed ($p < 0.001$, r = 0.52) in increased PET-OEF group (n = 8). The linear regression line was $y = 0.80\,x + 16.69$. In contrast, the correlation was also significant but weak ($p = 0.006$, r = 0.15) in preserved PET-OEF group (n = 18), with the linear regression line of $y = 0.23\,x + 43.58$.

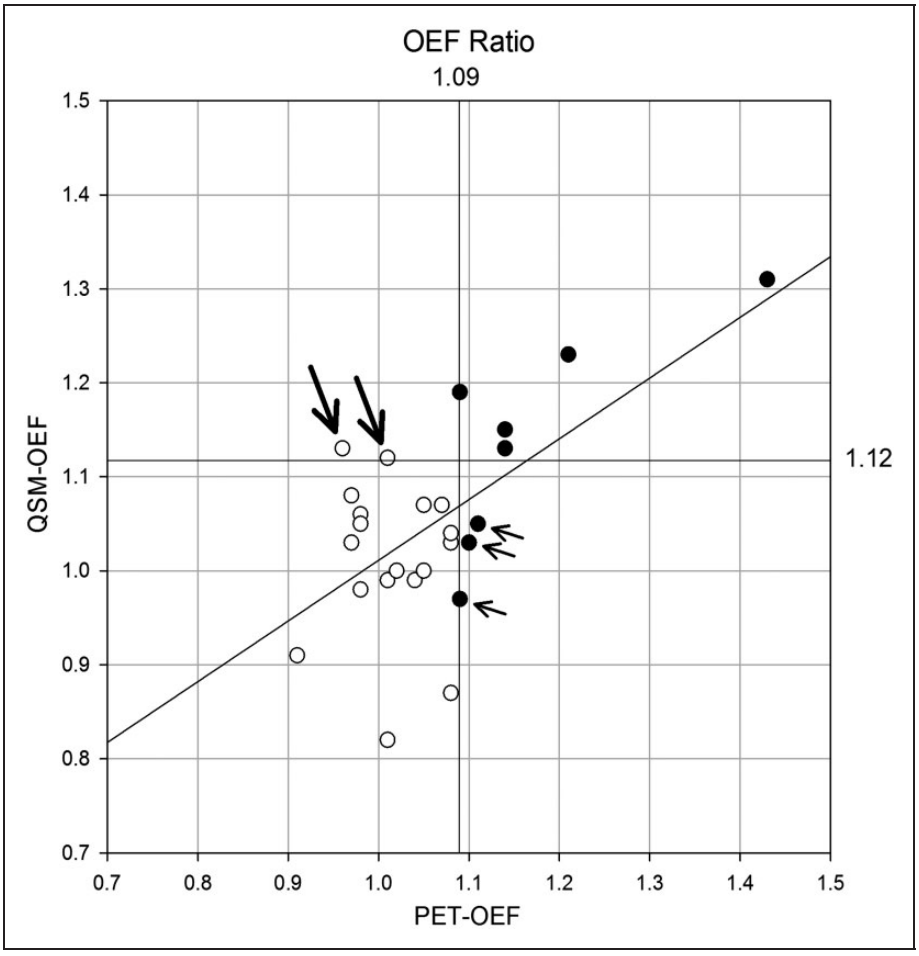

Figure 3. Relationship of oxygen extraction fraction (OEF) ratio. Scatter plot of OEF ratio is shown. Upper limit of normal ranges, defined as mean + 2 SD of normal data, are 1.09 for PET-OEF and 1.12 for QSM-OEF, respectively. Eight patients have significant increase in PET-OEF (•) and others have normal PET-OEF (○). Three patients have false-negative in QSM-OEF (small arrows). Among seven patients who had significant increase in QSM-OEF, five have also significant increase in PET-OEF (true-positive), and two does not have increase in PET-OEF (false-positive, large arrows). There is a significant and moderate correlation between QSM-OEF and PET-OEF ($p < 0.001$ and $r = 0.62$). The regression line is also shown ($y = 0.65\ x + 0.36$).

The ICC of two normal subjects were 0.80 and 0.84, respectively, which indicated moderate correlation.

Discussion

In this work we introduced the first direct comparison between QSM-OEF and PET-OEF measurements in a patient population. We observed good correlation between QSM-OEF and PET-OEF at the hemispheric level (OEF ratio), and significantly better local (intra-section) correlation was observed in patients with increased OEF than preserved OEF. Therefore, we suggest that OEF increases in affected hemispheres in patient groups such as those with unilateral chronic major cerebral artery steno-occlusive disease can be diagnosed with QSM-OEF. Although currently PET is considered to be the gold standard method for OEF measurement, there are some significant drawbacks with the technique, such as limited availability of PET scanners, considerable radiation exposure, which may prevent the potential for repeat scans, and the long scan time that is required. As a result, clinical application of OEF measurement by PET is limited, especially for acute stroke patients. In contrast, MRI is widely available in most stroke centers, and MR examinations of stroke patients are less invasive, and are common clinical practice in most countries. Therefore, OEF measurement using MRI can be beneficial for the management of patients with ischemic stroke as well as chronic major cerebral artery steno-occlusive disease.

Although the QSM approach shares some similarity with previously documented MRI-based OEF quantification methods in that the OEF quantification is based on local concentration of deoxy-Hb, the QSM approach has several advantages, which suggest that

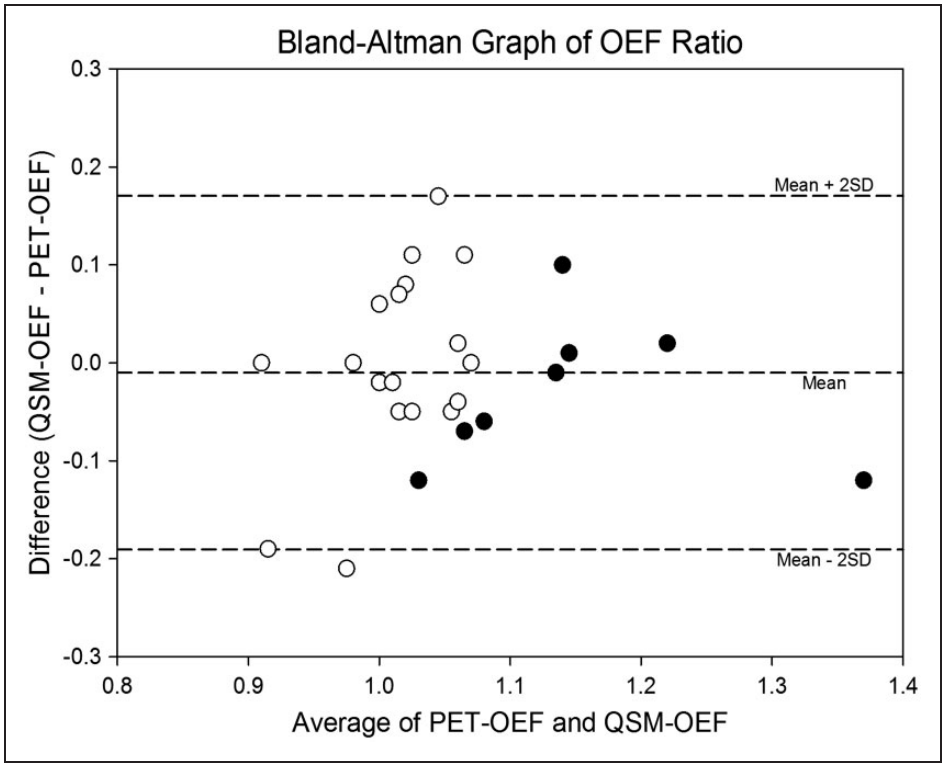

Figure 4. Bland-Altman graph of oxygen extraction fraction (OEF) ratio. Most of the data are within mean ± 2 SD, and no systemic bias is noted. Eight patients have significant increase in PET-OEF (●) and others have normal PET-OEF (○).

Table 3. Local (intra-section) correlation between QSM-OEF and PET-OEF.

		Number of patients	Correlation coefficients		
			mean	±	SD
PET-OEF	Increased	8	0.31	±	0.28
	Preserved	18	0.05	±	0.26
	All	26	0.13	±	0.29

PET: positron emission tomography; OEF: oxygen extraction fraction; QSM: quantitative susceptibility mapping.

this may be the most viable MRI-based alternative to PET OEF. Previous MRI methods utilizing T2*/T2' shortening or phase shift due to susceptibility effect of deoxy-Hb[5,6] have potential inaccuracy due to the presence of other paramagnetic substances in brain tissue that cause spin dephasing, and therefore may alter T2*/T2' relaxation times and the subsequent accuracy of OEF values. This possible inaccuracy is avoided by using the phase-based method, whereby venous phase values are measured after image segmentation of the veins is performed,[14] thus avoiding contamination by paramagnetic substances other than deoxy-Hb. This method is expected to measure OEF changes with greater sensitivity than the T2* or T2' approach; however, absolute quantification of OEF is not possible due to the orientation of the measured vasculature, which in addition to deoxy-Hb also affects the measured local phase value of the vein. It is possible to negate this problem by acquiring two scans to eliminate the effects of vessel geometry on the measured phase value in the veins, but in doing so only a relative change in OEF between two acquisitions can be measured,[14] not an absolute value of OEF, which is more desirable for clinical application. In contrast, QSM is a technique to calculate quantitative magnetic susceptibility without the effects associated with the geometry of the measured veins,[15] thereby allowing absolute quantification of OEF from a single scan. The QSM method may also have some advantages over the previously reported spin tagging approach to OEF measurement,[9,10] which is similar in principle to the well-documented MRI arterial spin labeling (ASL) technique for measuring cerebral blood flow, with the exception that in this case, venous rather than arterial blood is magnetically labeled to extract T2 relaxation measurements from the vein. This approach, while successfully demonstrated in healthy subjects with normal cerebrovasculature, may not be suitable for clinical populations such as ischemic patients, where reduced velocity of blood

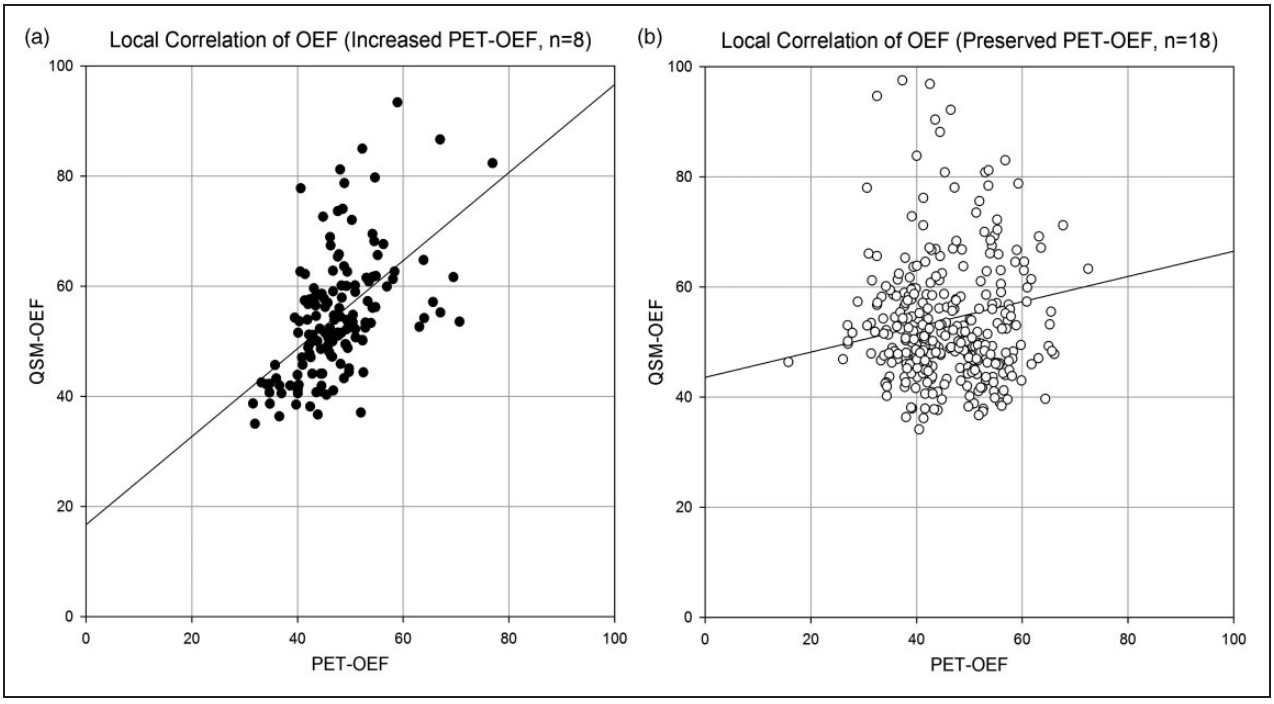

Figure 5. Local correlation between PET-OEF and QSM-OEF. Scatter plot of PET-OEF and QSM-OEF are shown for all ROI data (18 ROIs for each patient), with increased PET-OEF patients ($n = 8$, a), and preserved PET-OEF patients ($n = 18$, b). In increased PET-OEF group, significant and moderate correlation is observed ($p < 0.001$, $r = 0.52$), and the linear regression line is $y = 0.80\ x + 16.69$. In contrast, the correlation is also significant but weak ($p = 0.006$, $r = 0.15$) in preserved PET-OEF group, with the linear regression line of $y = 0.23\ x + 43.58$) .

flow may cause excessive T1 relaxation of labeled venous blood, before image acquisition can be performed.

Based on the comparison between the various MRI-based methods for measurement of OEF in clinical populations, currently the QSM method appears to be the most viable approach. Despite this, however, there are still some potential sources for inaccuracy with this approach, which require acknowledgment. In this study for example, we observed good correlation between QSM-OEF and PET-OEF at the hemispheric level; however, the local correlation was not high enough, even in patients with increased OEF. This may be related to the fact that calculation of local OEF values depends on the degree of partial volume averaging and segmentation of veins, as well as the concentration of deoxy-Hb. As such, improvement in the quality or resolution of the source image for QSM analysis to reveal more detail regarding the presence and geometry of veins will most likely lead to improvement in the accuracy of local OEF calculation. Furthermore, optimization of scanning parameters and QSM post-processing may also lead to more accurate quantification of OEF.

This study also faced some limitations in regard to the post-processing of OEF maps. Most notably the spatial resolution of the OEF map was not sufficient. This issue relates to the size of VOI of venous extraction, whereby if a higher spatial resolution is desired in the OEF map, then the size of VOI should decrease proportionally. However, this leads to greater inhomogeneity across the OEF map because the amount of venous pixels in the VOI decreases. In this event, even an accurate local evaluation of OEF may be difficult with the increase in spatial resolution. As such, obtaining an accurate balance between homogeneity of the OEF map with sufficient inclusion of venous pixels within a VOI is one of the challenges faced using the post-processing method for OEF quantification.

Additionally, the requirement that patients with a past history of hemorrhage should be excluded due to potential hemosiderin deposition in brain tissue, which can affect susceptibility values in QSM, is an obvious limitation. Similarly, the necessity to exclude slices, which included basal ganglia due to susceptibility effects of iron deposition, is another drawback. However, the development of a more sophisticated venous extraction method for OEF quantification may minimize these issues. Lastly, values of QSM-OEF depend on partial volume averaging of the veins. In this study we applied a correction factor for partial volume effects; however, the actual value of this

factor varies slightly on a vessel-by-vessel basis and is therefore difficult to accurately determine. The fact that QSM-OEF values were significantly larger than PET-OEF values is a concern. However, disregarding the absolute values of QSM-OEF, even the relative increase of OEF in affected hemispheres can be diagnosed by QSM-OEF, which correlates well with the equivalent PET-OEF images.

In conclusion, OEF measurement and map creation using QSM was feasible. Good correlation was achieved between QSM-OEF and PET-OEF in the identification of elevated OEF in affected hemispheres of patients with unilateral chronic steno-occlusive disease, although QSM-OEF values were larger than PET-OEF.

Funding

The authors disclosed receipt of the following financial support for the research, authorship, and/or publication of this article: This work was supported in part by a Grant-in-Aid for Strategic Medical Science Research from the Ministry of Education, Culture, Sports, Science and Technology of Japan, and by the Japan Society for the Promotion of Science (JSPS) through the ''Funding Program for Next Generation World-Leading Researchers (NEXT Program)'' initiated by the Council for Science and Technology Policy (CSTP).

Declaration of conflicting interests

The authors declared no potential conflicts of interest with respect to the research, authorship, and/or publication of this article.

References

1. Gibbs JM, Wise RJ, Leenders KL, et al. Evaluation of cerebral perfusion reserve in patients with carotid-artery occlusion. *Lancet* 1984; 1: 310–314.
2. Baron JC, Bousser MG, Rey A, et al. Reversal of focal ''misery-perfusion syndrome'' by extra-intracranial arterial bypass in hemodynamic cerebral ischemia. A case study with 15O positron emission tomography. *Stroke* 1981; 12: 454–459.
3. Grubb RL Jr, Derdeyn CP, Fritsch SM, et al. Importance of hemodynamic factors in the prognosis of symptomatic carotid occlusion. *JAMA* 1998; 280: 1055–1060.
4. Yamauchi H, Higashi T, Kagawa S, et al. Is misery perfusion still a predictor of stroke in symptomatic major cerebral artery disease? *Brain* 2012; 135: 2515–2526.
5. An H and Lin W. Quantitative measurements of cerebral blood oxygen saturation using magnetic resonance imaging. *J Cereb Blood Flow Metab* 2000; 20: 1225–1236.
6. An H, Lin W, Celik A, et al. Quantitative measurements of cerebral metabolic rate of oxygen utilization using MRI: a volunteer study. *NMR Biomed* 2001; 14: 441–447.
7. Menon RG, Walsh EG, Twieg DB, et al. Snapshot MR technique to measure OEF using rapid frequency mapping. *J Cereb Blood Flow Metab* 2014; 34: 1111–1116.
8. He X and Yablonskiy DA. Quantitative BOLD: mapping of human cerebral deoxygenated blood volume and oxygen extraction fraction: default state. *Magn Reson Med* 2007; 57: 115–126.
9. Bolar DS, Rosen BR, Sorensen AG, et al. QUantitative Imaging of eXtraction of oxygen and TIssue consumption (QUIXOTIC) using venular-targeted velocity-selective spin labeling. *Magn Reson Med* 2011; 66: 1550–1562.
10. Lu H and Ge Y. Quantitative evaluation of oxygenation in venous vessels using T2-Relaxation-Under-Spin-Tagging MRI. *Magn Reson Med* 2008; 60: 357–363.
11. Xie S. MR OEF imaging in MELAS. *Meth Enzymol* 2014; 547: 433–444.
12. An H, Sen S, Chen Y, et al. Noninvasive measurements of cerebral blood flow, oxygen extraction fraction, and oxygen metabolic index in human with inhalation of air and carbogen using magnetic resonance imaging. *Trans Stroke Res* 2012; 3: 246–254.
13. Haacke EM, Lai S, Reichenbach JR, et al. In vivo measurement of blood oxygen saturation using magnetic resonance imaging: a direct validation of the blood oxygen level-dependent concept in functional brain imaging. *Hum Brain Mapp* 1997; 5: 341–346.
14. Zaitsu Y, Kudo K, Terae S, et al. Mapping of cerebral oxygen extraction fraction changes with susceptibility-weighted phase imaging. *Radiology* 2011; 261: 930–936.
15. Liu J, Liu T, de Rochefort L, et al. Morphology enabled dipole inversion for quantitative susceptibility mapping using structural consistency between the magnitude image and the susceptibility map. *Neuroimage* 2012; 59: 2560–2568.
16. Liu T, Liu J, de Rochefort L, et al. Morphology enabled dipole inversion (MEDI) from a single-angle acquisition: comparison with COSMOS in human brain imaging. *Magn Reson Med* 2011; 66: 777–783.
17. Xu Y and Haacke EM. The role of voxel aspect ratio in determining apparent vascular phase behavior in susceptibility weighted imaging. *Magn Reson Imaging* 2006; 24: 155–160.
18. Vignes JR, Dagain A, Guerin J, et al. A hypothesis of cerebral venous system regulation based on a study of the junction between the cortical bridging veins and the superior sagittal sinus. Laboratory investigation. *J Neurosurg* 2007; 107: 1205–1210.
19. Haacke EM, Tang J, Neelavalli J, et al. Susceptibility mapping as a means to visualize veins and quantify oxygen saturation. *J Magn Reson Imaging* 2010; 32: 663–676.
20. van Zijl PC, Eleff SM, Ulatowski JA, et al. Quantitative assessment of blood flow, blood volume and blood oxygenation effects in functional magnetic resonance imaging. *Nat Med* 1998; 4: 159–167.
21. Lammertsma AA and Jones T. Correction for the presence of intravascular oxygen-15 in the steady-state technique for measuring regional oxygen extraction ratio in the brain: 1. Description of the method. *J Cereb Blood Flow Metab* 1983; 3: 416–424.
22. Kudo K, Sasaki M, Ogasawara K, et al. Difference in tracer delay-induced effect among deconvolution

algorithms in CT perfusion analysis: quantitative evaluation with digital phantoms. *Radiology* 2009; 251: 241–249.
23. Kudo K, Sasaki M, Ostergaard L, et al. Susceptibility of T(max) to tracer delay on perfusion analysis: quantitative evaluation of various deconvolution algorithms using digital phantoms. *J Cerebral Blood Flow Metabol* 2011; 31: 908–912.
24. Ishigaki D, Ogasawara K, Yoshioka Y, et al. Brain temperature measured using proton MR spectroscopy detects cerebral hemodynamic impairment in patients with unilateral chronic major cerebral artery steno-occlusive disease: comparison with positron emission tomography. *Stroke* 2009; 40: 3012–3016.